

Fermi enhancement and breakdown of the parity selection rule in the luminescence spectra of GaAs/Al_xGa_{1-x}As modulation-doped quantum wells

Y. F. Chen, L. Y. Lin, and J. L. Shen

Department of Physics, National Taiwan University, Taipei, Taiwan, Republic of China

D. W. Liu

Department of Physics, Florida Atlantic University, Boca Raton, Florida

(Received 27 April 1992)

We report the results of an investigation of the optical properties of modulation-doped GaAs/Al_xGa_{1-x}As multiple quantum wells with sheet-carrier concentration up to $1.8 \times 10^{12} \text{ cm}^{-2}$. Photoluminescence and resonant Raman-scattering techniques have been used as complementary tools for the characterization of the intersubband transition. A two-band model of the two-dimensional plasma gives good agreement between the photoluminescence excitation data and Hall measurements. We point out that the large breakdown of the parity selection rule of the optical matrix element in the photoluminescence spectra is due to the localization of photogenerated holes at the heterointerface, which lifts the k -selection restriction. The enhancement in the photoluminescence intensity at the Fermi edge results from the strong correlation and multiple scattering of electrons near the Fermi edge by the localized holes.

I. INTRODUCTION

In addition to the enhancement in the carrier mobility through the spatial separation of the dopant atoms and the mobile electrons, modulation-doped quantum wells possess unique properties for the study of many important physical phenomena such as (1) band-gap renormalization due to many-body effects,¹ (2) the Burstein-Moss shift due to band filling,² (3) Fermi-edge singularity due to electron-hole multiple scattering,³ (4) quenching of excitons due to phase-space filling and screening,⁴ and (5) carrier-induced changes in refractive index.⁵ Thus, modulation-doped quantum wells have stimulated many research works not only for their technological applications but also for their academic interests. Recently, Pinczuk *et al.*⁶ and Liu, Brody, and Chi⁷ observed a large breakdown of the parity selection rule of the optical matrix element of photoluminescence spectra in GaAs/Al_xGa_{1-x}As modulation-doped quantum wells when a large amount of carriers are introduced into the wells. They also observed a large band-gap shrinkage due to particle correlations. A theoretical investigation has been followed,⁸ but the unexpectedly large breakdown of the parity selection rule is still unresolved. Also, a feature in the high-energy edge of the spectra remains unexplained.

This paper addresses the optical investigation of the electronic transitions in GaAs/Al_xGa_{1-x}As modulation-doped quantum wells. Photoluminescence measurements with the pumping photon energies below and above the band gap of the Al_xGa_{1-x}As barrier layer, photoluminescence excitation, and the resonant Raman scattering have been performed in order to probe the optical response of the multiple quantum wells confining a dense electron plasma. From our data we show that the photoluminescence emission and excitation techniques

can be used to determine the concentration of two-dimensional plasma. The resonant Raman scattering can serve as an auxiliary tool to confirm the intersubband transition. In addition, we point out that the large breakdown of the parity selection rule is due to the localization of photogenerated holes at heterointerface, which lifts the k -selection rule. We also show that previously unexplained feature in the high-energy side of the photoluminescence spectra can be attributed to the so-called Fermi-edge singularity, which is a consequence of many-body interactions between electrons and localized holes generated by the pumping source.

II. EXPERIMENT

The investigated samples are modulation-doped n -type GaAs/Al_{0.3}Ga_{0.7}As multiple quantum wells grown on a semi-insulating GaAs (100) substrate at a temperature of about 650 °C. A GaAs buffer layer was grown first, followed by the required number of alternating layers of Al_{0.3}Ga_{0.7}As and GaAs. In these modulation-doping structures, only Al_xGa_{1-x}As layers are intentionally doped, leaving the GaAs layers essentially free of impurities. Electrons transfer from the higher-energy conduction band of the Al_xGa_{1-x}As barrier layer to the lower-energy band of the GaAs layer achieving spatial separation of electrons from their parent ionic donors. Thus, a two-dimensional (2D) charge plasma is formed inside the GaAs layer. Our multiple-quantum-well heterostructures consist of 15 periods with a typical well width of 20 nm, undoped Al_{0.3}Ga_{0.7}As spacer layer with thickness 5 nm adjacent to a Si-doped barrier layer, and a Si-doped Al_{0.3}Ga_{0.7}As barrier width of 50 nm. From the Hall measurements, sample *A* has a carrier concentration of $1.8 \times 10^{12} \text{ cm}^{-2}$ and a mobility of $8 \times 10^4 \text{ cm}^2/\text{V sec}$ at 5 K, and sample *B* has a carrier concentration of 1.5×10^{12}

cm^{-2} and a mobility of $8.5 \times 10^4 \text{ cm}^2/\text{V sec}$. The sample was cut with a wire saw so that its long axis was parallel to (100) to facilitate mounting, strain free, in an exchange liquid-helium cryostat. A standard Spex 1401 1-m double-grating spectrometer equipped with a cooled GaAs photomultiplier was used to obtain the spectra. The excitation source consisted of a dye laser pumped by a 5-W all-lines krypton-ion laser. For the resonant Raman measurements, Rhodamine-101 was employed as a lasing medium for the dye laser in order to match the energy near the $E_0 + \Delta_0$ spin-orbit split optical band gap of the GaAs wells, at approximately 1.9 eV. For the photoluminescence excitation measurements, the birefringent filter unit in the dye laser cavity was coupled to a synchronous stepping motor system to provide continuous varying excitation energies while the spectrometer was set at a fixed wavelength. Oxazine 750 dissolved in DMSO (dimethylsulfoxide) was employed, giving a variable excitation energy from 1.50 to 1.64 eV. The laser beam was polarized along (110) and entered the sample along (001) nearly normal to the layers. An angle of incidence on the sample of 15° resulted in a nearly back-scattering geometry inside the sample.

III. RESULTS AND DISCUSSION

Typical photoluminescence spectra of our samples using an argon-ion laser with 2.54 eV measured at 5 K are shown in Fig. 1. Four dominant peaks, indicated as

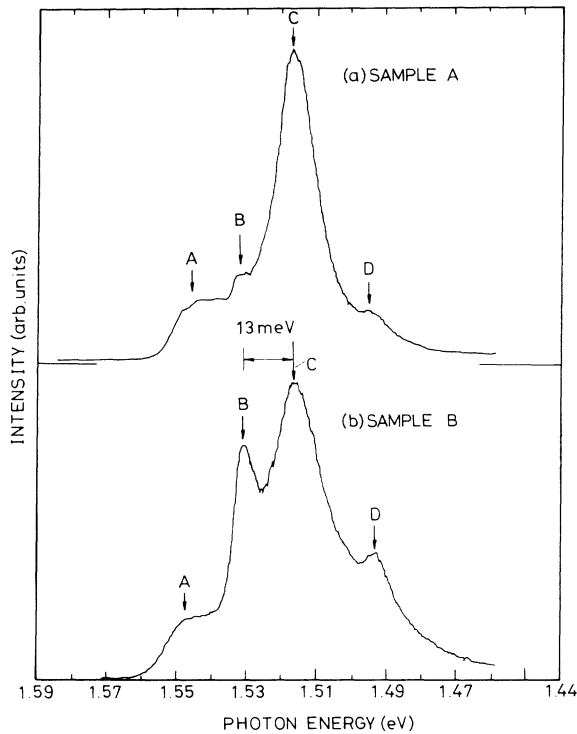


FIG. 1. Photoluminescence spectra of modulation-doped GaAs/ $\text{Al}_{0.3}\text{Ga}_{0.7}\text{As}$ multiple quantum wells for samples *A* and *B* with a carrier concentration of $1.8 \times 10^{12} \text{ cm}^{-2}$ and $1.5 \times 10^{12} \text{ cm}^{-2}$, respectively, measured at 5 K with an excitation energy of 2.54 eV.

A–D, are observed. When the pumping source is replaced by a HeNe laser, we obtain the same spectrum (not shown). According to the previous investigations,^{6,7} the peak *D* at energy 1.494 eV is due to the carbon impurities in the GaAs substrate. The largest peak *C* at energy 1.512 eV is associated with a $\Delta n = 0$ transition, i.e., the ground conduction subband to ground-state heavy-hole subband. In order to clarify the origins of the higher-energy peaks, the resonant Raman scattering is incorporated in the analysis.

The resonant Raman investigations on the multiple quantum wells have been studied in detail previously.^{9–11} The excitation energy of the $E_0 + \Delta_0$ spin-orbit optical band gap of the GaAs wells was employed because it leads to the enhanced scattering mechanisms by electrons. In addition, the weaker Raman signals can be clearly separated from the large photoluminescence intensities to avoid signal contamination. In our Raman measurement, the configuration of orthogonal polarization has been used, in which the incident and scattered light polarizations are orthogonal. It has been shown that there is no depolarization field effect in this arrangement because of the spin-flip between initial and final states.⁹ Therefore, the spectrum represents a single-particle intersubband excitation. Thus, the peak at 13 meV in the Raman spectrum shown in Fig. 2 is the energy separation between the first and second conduction subband, which is in good agreement with the previous calculation and the experimental measurements.^{8,9} This energy is in excellent agreement with the separation between the two emission bands indicated as peaks *C* and *B* in Fig. 1. Thus, the peak *B* in Fig. 1 could be due to the $\Delta n = 1$ transition from the first excited conduction subband to ground valence subband states. If this assignment is correct, we will obtain a large breakdown of the parity selection rule of the optical matrix element in the quantum wells. For example, from the line-shape

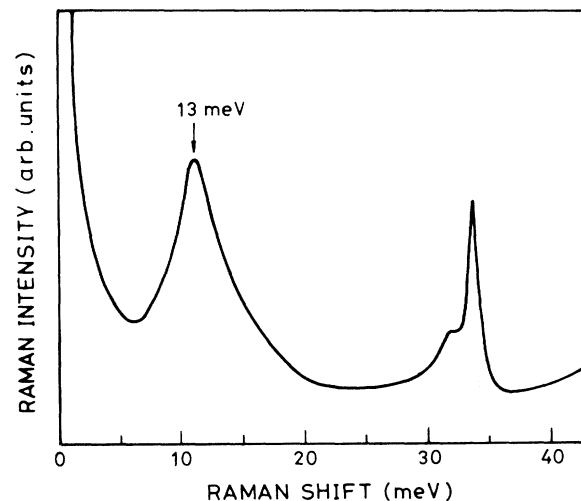


FIG. 2. Raman-scattering spectrum of sample *A* with crossed polarization geometry measured at 5 K and with an excitation energy of 1.9 eV.

analysis Pinczuk *et al.*⁶ obtained the ratio between parity-allowed and parity-forbidden optical matrix elements having a value of 0.6. However, according to the theoretical calculation by Bauer and Ando,⁸ the transition from the second conduction subband to the ground-state heavy-hole subband is forbidden, even if the many-body effects are included. Although breakdown of the parity selection rule has been observed in light-scattering spectra¹² and in luminescence from high-density photoexcited plasma,¹³ the unexpectedly large breakdown observed here is still an open question. The Raman spectrum in Fig. 2 shows a peak at 34 meV which is most likely the GaAs-like mode related to the alloy.⁷

Before turning to explain the large breakdown of the parity selection rule and the origin of the peak *A*, as shown in Fig. 1, let us now examine our photoluminescence excitation spectrum and the photoluminescence spectra for the pumping source with photon energy below the band gap of $\text{Al}_{0.3}\text{Ga}_{0.7}\text{As}$ barrier layers. One representative photoluminescence excitation spectrum on sample *A* (same sample as in Fig. 2) at 5 K is shown in Fig. 3, where the spectrometer was set on the band-gap energy $E_0 = 1.512$ eV. The absorption edge, $E_{\text{abs}} = 1.5557$ eV, from this spectrum was determined, at which the intensity went to one-half of its maximum value. The difference between the band-gap energy and the absorption edge is due to the Burstein-Moss Fermi energy shift E_F . In the parabolic approximation and for *n*-type doping the energy spacing between E_{abs} and E_0 , which is at the energy of the attenuated laser line in Fig. 3, can be described by⁶

$$E_{\text{abs}} - E_0 = E_F \left(1 + m_e^* / m_h^*\right), \quad (1)$$

where m_e^* and m_h^* are the effective masses for the conduction and valence bands, respectively. For the occupation of two conduction subbands in two-dimensional plasma the Fermi energy E_F , and the plasma density N , are related by¹⁴

$$\begin{aligned} N &= (m_e^* / \pi \hbar^2) E_F + (m_e^* / \pi \hbar^2) (E_F - E_{01}) \\ &= (m_e^* / \pi \hbar^2) (2E_F - E_{01}), \end{aligned} \quad (2)$$

where E_{01} is the energy separation between the first and second conduction subband. Thus the two-dimensional electron density N can be determined from the energy separation between E_{abs} and E_0 obtained in the corresponding photoluminescence excitation spectrum. Adopting $m_e^* = 0.068m_0$, $m_h^* = 0.39m_0$ (m_0 is free-electron mass), and $E_{01} = 13$ meV, we obtain the plasma density $N = 1.76 \times 10^{12} \text{ cm}^{-2}$. This value is in good agreement with the two-dimensional electron-gas concentration $N = 1.82 \times 10^{12} \text{ cm}^{-2}$ obtained from the Hall-effect measurement. Therefore, this agreement not only demonstrates that the photoluminescence emission and excitation techniques can be used to determine the carrier concentration, but also provides the evidence to support the assignment of the peaks *B* and *C* in Fig. 1.

Figure 4 shows a typical photoluminescence spectrum of our samples when the pumping photon energy is below the band gap of the $\text{Al}_{0.3}\text{Ga}_{0.7}\text{As}$ barrier. Several

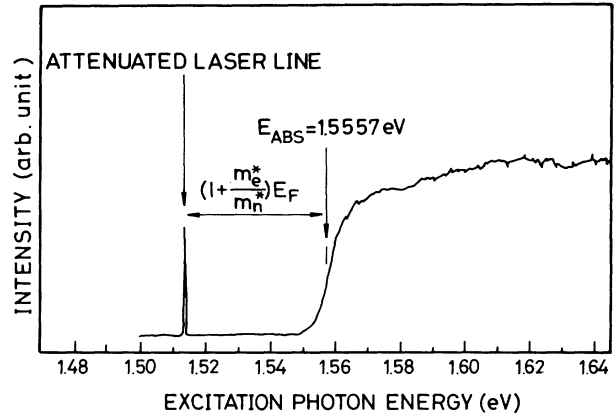


FIG. 3. Photoluminescence excitation spectrum of sample *A* measured at 5 K by setting the spectrometer on the band-gap energy of 1.5125 eV.

different pumping photon energies from 1.56 to 1.60 eV have been performed, but we always obtain the same spectrum (not shown here). Comparing Figs. 1 and 4, we can see that the spectra are quite different. In Fig. 4, the dominant emissions are due to the transitions related to carbon impurities and the ground conduction subband to the ground-state heavy-hole subband. The peaks *A* and *B* shown in Fig. 1 completely disappear in Fig. 4. In addition, Fig. 4 shows a small shoulder at 1.515 eV.

We now provide the explanation for the large breakdown of the parity selection rule of the optical transition matrix element, the unidentified feature of peak *A* shown in Fig. 1, and the striking difference of the photoluminescence spectra for the pumping source with photon energies below and above the band gap of the $\text{Al}_{0.3}\text{Ga}_{0.7}\text{As}$ barrier. Since the conditions for the measurements of Figs. 1 and 4 are the same except for the pumping photon energy, there is a possibility that the excess features in Fig. 1 are due to the emission from the $\text{Al}_{0.3}\text{Ga}_{0.7}\text{As}$ layers. However, from the study of heavily doped

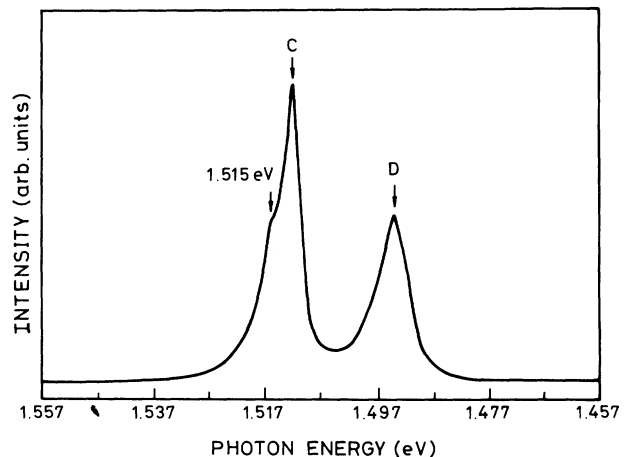


FIG. 4. Photoluminescence spectrum of sample *A* measured at 9.5 K with an excitation energy of 1.57 eV.

$\text{Al}_x\text{Ga}_{1-x}\text{As}$,¹⁵ even when there is a broadband of emission below the band gap, the emission energy is far below 1.55 eV. Therefore, the possibility that the peaks *A* and *B* in Fig. 1 might arise from the $\text{Al}_{0.3}\text{Ga}_{0.7}\text{As}$ barrier can be excluded.

We attribute these features to the localization of photo-generated nonequilibrium holes by the inherent roughness of the $\text{GaAs}/\text{Al}_{0.3}\text{Ga}_{0.7}\text{As}$ heterointerface. This kind of localization of nonequilibrium holes relaxes the *k*-selection rule and allows them to recombine with electrons at all occupied *k* states up to the Fermi edge. The intensity enhancement near the Fermi edge indicated as peak *A* in Fig. 1 resembles the expected characteristics of Fermi-edge singularity, which results from the strong correlation and multiple scattering of electrons near the Fermi edge by the localized holes. The difference in the photoluminescence spectra between the pumping sources with photon energies above and below the band gap of the $\text{Al}_{0.3}\text{Ga}_{0.7}\text{As}$ barrier is a consequence of different penetration depths of the exciting light. For excitation at 2.54 eV, the light is strongly absorbed both in the $\text{Al}_{0.3}\text{Ga}_{0.7}\text{As}$ and GaAs layers. The penetration depth $1/\alpha$, where α denotes the absorption coefficient, amounts to 20 nm for GaAs .¹⁶ Therefore holes are mainly photoexcited in the region of the first period below the sample surface and get trapped close to the topmost heterointerface. This causes an additional asymmetry of the confining potentials, and leads to a modification of the electron-hole wave-function overlap favoring the observation of the peaks *A* and *B* in Fig. 1. In contrast, for excitation at energy below the band gap of the $\text{Al}_{0.3}\text{Ga}_{0.7}\text{As}$ barrier, holes are photogenerated at both sides of the GaAs well at about equal concentrations because of the much larger penetration depth of light. Therefore the resulting potential is expected to be more symmetric than in the previous case, and emission processes occur at the subband energy corresponding to electronic transitions at $k=0$. The above argument has been used to explain the photoluminescence spectra in δ -doped GaAs by Wagner, Ruiz, and Ploog¹⁷ when the excitation energies are below or above the band gap of the barrier layer. However, in the previously investigated samples,¹⁷ the Fermi edges are below the second subband; hence they did not observe the breakdown of parity selection rule.

In our interpretation, it is clearly that the localization of photo-generated holes plays a key role in determining the photoluminescence spectra of the samples under our investigation. Actually, the importance of localization of photo-generated carriers has been demonstrated in many photoluminescence spectra recently. An outstanding example is that all the observations of Fermi-edge singularity in luminescence spectra have to require the localized carriers as discussed below.¹⁸ In addition, the radiative recombination due to the localization of photo-generated holes has been observed in Si metal-oxide-semiconductor field-effect transistors,¹⁹ as well as $\text{GaAs}/\text{Al}_x\text{Ga}_{1-x}\text{As}$,²⁰ $\text{Ga}_x\text{In}_{1-x}\text{As}/\text{InP}$ (Ref. 3), and $\text{Ga}_x\text{In}_{1-x}\text{As}/\text{Al}_y\text{In}_{1-y}\text{As}$ (Ref. 18) modulation-doped quantum wells and heterostructures. By assuming a *k*-nonconserving transition due to the localized carriers, Zhang, Cingolani, and Ploog²¹ determined the electron

concentration by simply measuring the luminescence energy bandwidth. Therefore, the appearance of the localization of photogenerated carriers may be considered as a common feature in most semiconductor heterostructures.

The convincing observation of the Fermi-edge singularity in semiconductor luminescence spectra by Skolnick *et al.*³ has stimulated many research works on this problem. This observation is a direct manifestation of the enhanced multiple electron-hole scattering rate for electrons close to the Fermi edge in an electron plasma of high density. It is analogous to the observation in the soft-x-ray emission and absorption spectra of metals,²² where it is referred to as the many-body x-ray edge singularity. Although holes in semiconductors are mobile in contrast to the atomic core-level electrons in metal, the Fermi-edge anomaly is caused because the Fermi wave number is smaller than in metals. However, the enhancement in the photoluminescence spectra near the Fermi edge is difficult to explain, if we consider the *k* conservation in the transition from the conduction band near the Fermi level to the bottom of the valence band unless a kind of hole localization is taken into account. It is found that in order to observe the Fermi-edge singularity, the localization of the holes must result in positively charged centers.¹⁸ These centers attract the electrons around them through Coulomb interaction. Such scattering processes for electrons with a *k* state far below the Fermi edge are suppressed by the exclusion principle, so that only electrons close to the Fermi edge are

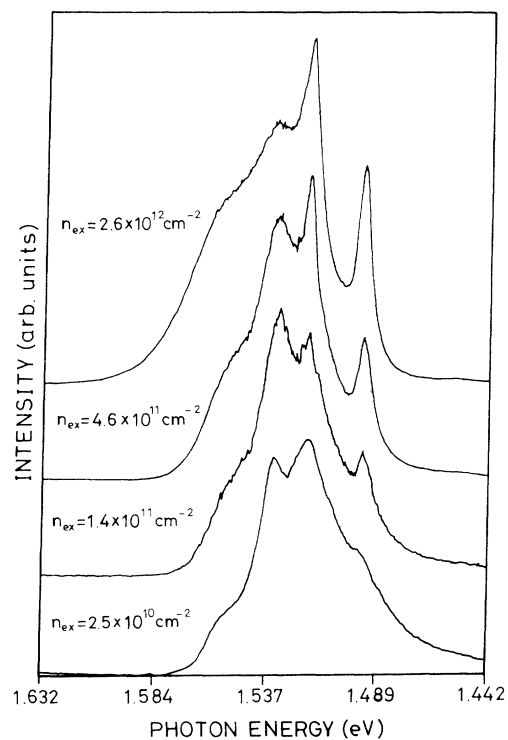


FIG. 5. Excitation-intensity-dependent photoluminescence spectra of sample *B* measured at 6.5 K with an excitation energy of 2.54 eV.

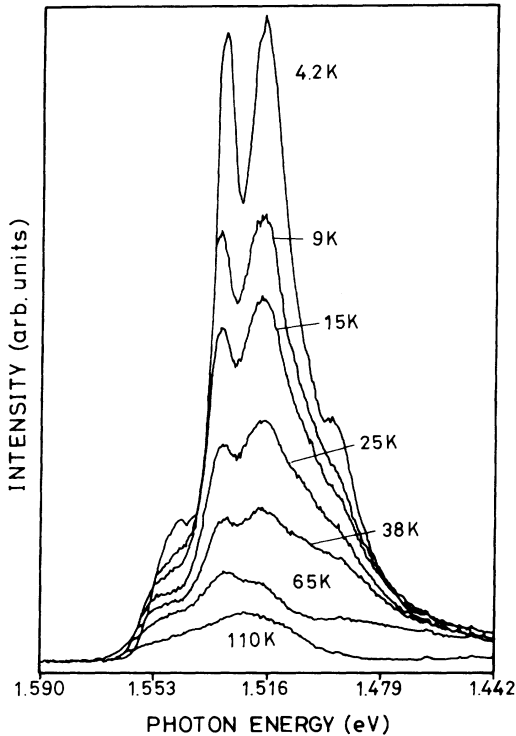


FIG. 6. Photoluminescence spectrum of sample *B* with an excitation energy of 2.54 eV as a function of temperature.

affected. Due to the strong electron-electron correlation, the scattering is multiple electron-hole scattering and results in the enhancement of the oscillator strength near the Fermi edge. If the localization of the photogenerated holes results in electrically neutral centers, even it can cause radiative recombination for all electrons, but no enhancement is induced for the oscillator strength of the recombination of electrons near the Fermi edge.

Inspecting Fig. 1, except for the fact that peak *A* is located near the Fermi edge, which is obtained from the absorption edge of the photoluminescence excitation, we also found that the energy difference ΔE between peaks *A* and *C* is almost equal to the Fermi energy 37.5 meV obtained from Eq. (1). Therefore, the photoluminescence spectrum basically represents the distribution of the two-dimensional electrons from the bottom of the conduction band to the Fermi level. Thus, peak *A* could be due to the Fermi-edge singularity, as discussed above. The assignment of this peak gets further support from excitation-intensity-dependent photoluminescence spectra shown in Fig. 5. First, the intensity of the recombination involving this peak increases with increasing excitation intensity. Second, the high-energy edge of this peak shifts to higher energies with increasing excitation inten-

sity. The change in the intensity can be explained by an increase in the concentration of photogenerated holes trapped at the heterointerface, which is a prerequisite for the observation of the Fermi-edge singularity in the present samples. The energy shift of the high-energy cutoff, which represents the Fermi edge in the electron distribution, indicates a filling of the conduction subband with photogenerated electrons. In addition, the temperature-dependent photoluminescence spectra shown in Fig. 6 exhibit the expected behavior of the Fermi-edge singularity. When the temperature increases, the width of the luminescence line becomes broader on the high-energy side, reflecting the change of the electron distribution according to the Fermi statistics. As the temperature reaches 110 K, the enhancement disappears because of the thermal broadening of the Fermi edge.^{3,23} This behavior provides additional evidence for the existence of the Fermi-edge singularity in the luminescence spectra of the investigated samples and excludes the possibility that the luminescence comes from the recombination of electrons in the higher electron subband.²⁴ We thus have observed the Fermi-edge singularity in the photoluminescence spectra of samples with the Fermi edge in the second conduction subband. All the previous reports on the subject deal with the Fermi edge in the ground subband.²⁵⁻²⁷

IV. SUMMARY

Photoluminescence and resonant Raman-scattering techniques have been used as the complementary tools for the characterization of the intersubband transition in modulation-doped GaAs/Al_{0.3}Ga_{0.7}As quantum wells with the carrier concentration of $1.8 \times 10^{12} \text{ cm}^{-2}$. A two-band model of the two-dimensional plasma gives good agreement between the photoluminescence excitation data and Hall measurements. We have pointed out that the large breakdown of the parity selection rule of the optical matrix element in the photoluminescence spectra can be attributed to the localization of photogenerated holes at the heterointerface, which lifts the *k*-selection restriction. We have also demonstrated the Fermi-edge singularity in the photoluminescence spectra, which results from the strong correlation and multiple scattering of electrons near the Fermi edge by the localized holes. For excitation with photon energy below the band gap of the Al_{0.3}Ga_{0.7}As barrier, the radiative recombination is dominated by electronic transitions at $k=0$.

ACKNOWLEDGMENTS

We would like to thank Dr. Y. H. Chang for useful discussions. This work was partly supported by the National Science Council of the Republic of China.

¹D. A. Kleinman and R. C. Miller, Phys. Rev. B **32**, 2266 (1985).

²M. H. Meynadier, J. Orgonasi, C. Delalande, J. A. Brum, G. Bastard, M. Voos, G. Weimann, and W. Schlapp, Phys. Rev.

B **34**, 2482 (1986).

³M. Skolnick, J. M. Rorison, K. J. Nash, D. J. Mowbray, P. R. Tapster, S. T. Bass, and A. D. Pitt, Phys. Rev. Lett. **58**, 2130 (1987).

- ⁴D. S. Chemla, D. A. B. Miller, and J. Matsusue, *J. Opt. Soc. Am. B* **2**, 1155 (1985).
- ⁵H. Sakaki, H. Yoshimura, and T. Matsusue, *Jpn. J. Appl. Phys.* **26**, L1104 (1987).
- ⁶A. Pinczuk, J. Shan, R. C. Miller, A. C. Gossard, and W. Wiegmann, *Solid State Commun.* **50**, 735 (1984).
- ⁷D. W. Liu, E. M. Brody, and J. Chi, *J. Appl. Phys.* **65**, 726 (1989).
- ⁸G. E. W. Bauer and T. Ando, *Phys. Rev. B* **31**, 8321 (1985).
- ⁹J. E. Eucker, A. Pinczuk, D. S. Chemla, A. Gossard, and W. Wiegmann, *Phys. Rev. Lett.* **51**, 1293 (1983).
- ¹⁰E. Burstein, A. Pinczuk, and D. L. Mills, *Surf. Sci.* **98**, 451 (1980).
- ¹¹A. Pinczuk, H. L. Stormer, R. Dingle, J. M. Worlock, W. Wiegmann, and A. C. Gossard, *Solid State Commun.* **30**, 429 (1979); **32**, 1001 (1979); **36**, 43 (1980).
- ¹²A. Pinczuk and J. M. Worlock, *Surf. Sci.* **113**, 69 (1982).
- ¹³R. C. Miller, D. A. Kleinman, D. Munteanu, and W. T. Tsang, *Appl. Phys. Lett.* **39**, 1 (1981).
- ¹⁴G. Fishman, *Phys. Rev. B* **27**, 7611 (1983).
- ¹⁵P. L. Souza and E. V. K. Rao, *J. Appl. Phys.* **67**, 7013 (1990).
- ¹⁶M. Cardona and G. Harbeke, *J. Appl. Phys.* **34**, 813 (1962).
- ¹⁷J. Wagner, A. Ruiz, and K. Ploog, *Phys. Rev. B* **43**, 12134 (1991).
- ¹⁸Y. H. Zhang, N. N. Ledentsov, and K. Ploog, *Phys. Rev. B* **44**, 1399 (1991).
- ¹⁹I. V. Kukushkin and V. B. Timofeev, *Zh. Eksp. Teor. Fiz.* **93**, 1088 (1987) [*Sov. Phys. JETP* **66**, 613 (1987)].
- ²⁰I. V. Kukushkin, K. v. Klitzing, and K. Ploog, *Phys. Rev. B* **37**, 8509 (1988).
- ²¹Y. H. Zhang, R. Cingolani, and K. Ploog, *Phys. Rev. B* **44**, 5958 (1991).
- ²²T. A. Callcott, E. T. Arokawa, and D. L. Ederer, *Phys. Rev. B* **18**, 6622 (1978).
- ²³Y. H. Zhang, D. S. Jiang, R. Cingolani, and K. Ploog, *Appl. Phys. Lett.* **56**, 2195 (1990).
- ²⁴T. Rötger, J. C. Mann, P. Wyder, F. Meseguer, and K. Ploog, *J. Phys. (Paris Colloq.)* **48**, C5-389 (1987).
- ²⁵J. S. Lee, Y. Iwasa, and N. Miura, *Semicond. Sci. Technol.* **2**, 675 (1987).
- ²⁶S. Munnix, D. Bimberg, D. E. Mars, J. N. Miller, E. C. Lar-kins, and J. S. Harris, *Superlatt. Microstruct.* **6**, 369 (1989).
- ²⁷S. Haacke, R. Zimmermann, D. Bimberg, H. Kal, D. E. Hars, and J. N. Miller, *Phys. Rev. B* **45**, 1736 (1992).